Research Article

Alpha-tocopherol microspheres with cross-linked and acetylated inulin and their release profile in a hydrophilic model

Paula García[1], Juan Vega[1], Paula Jimenez[2], José Santos[3] and Paz Robert[1]

[1] Facultad de Ciencias Químicas y Farmacéuticas, Departamento de Ciencia de los Alimentos y Tecnología Química, Universidad de Chile, Santiago, Chile
[2] Facultad de Medicina, Departamento de Nutrición, Universidad de Chile, Santiago, Chile
[3] Facultad de Química, Departamento de Química-Física, Pontificia Universidad Católica de Chile, Santiago, Chile

Alpha-tocopherol (AT) was encapsulated with native (NIn), acetylated (AIn) or cross-linked (CIn) inulin (two degrees each) by spray-drying. A face central composite experimental design for each system (AT–NIn, AT–AIn_1, AT–AIn_2, AT–CIn_1, and AT–CIn_2) was evaluated to determine the influence of inlet air temperature and AT/coating material ratio on the AT encapsulation percentage (EP). The AT microspheres obtained under optimal conditions were characterized determining the AT EP, morphology and their release profile in a hydrophilic system. The AT encapsulating percentage reached values above 86% in all the systems studied. The acetylation and cross-linking of inulin improved slight but significantly the AT encapsulating percentage respect to native inulin. The release profiles showed biphasic behavior, being the first and second zone attributed to uncovered and encapsulated AT, respectively. The AT release was $< 15\%$ (0–540 min) from all AT-inulin microparticles, corresponding mainly to superficial AT release, following Higuchi model consistent with a diffusional mechanism. AT release rate constant from AT–NIn microspheres was significantly lower than those of AT–AIn and AT–CIn. The AT release pattern suggest that the microparticles could be applied in the design of functional foods, preserving the nutritional role of AT.

Keywords: Acetylated inulin / Alpha-tocopherol / Cross-linked inulin / Microencapsulation / Release profile

Received: March 13, 2012 / Revised: February 26, 2013 / Accepted: April 8, 2013

DOI: 10.1002/ejlt.201200109

1 Introduction

Alpha-tocopherol (AT) is well-known for its effective inhibition of lipid oxidation in food and biological systems. The antioxidant activity of AT is due to its ability to donate phenolic hydrogen to peroxyl radicals [1]. Therefore, AT is a potential functional additive for biological systems, decreasing the risk of diseases associated with oxidative stress, such as cardiovascular disease and cancer [2]. In addition, other biological activities, such as prevention of hypertension, type 2 diabetes, Alzheimer's [3], and strengthening immune function, have been reported [4]. The application of AT in food is limited due to its low stability (heat, oxygen, and light) and poor aqueous solubility (high hydrophobicity) [1]. To overcome these problems AT has been encapsulated in protective matrixes avoiding oxidation and increasing its shelf life [3, 5–8].

In recent years, encapsulation technology has increased importance in the food industry, particularly in the development of functional and healthy foods. The use of encapsulated AT as additive in foods should protect the active compound until the functional food is consumed, preserving its nutritional properties [9]. Without this protection, the AT would otherwise be exposed to adverse conditions in the food (pH, enzymes, and other food components). In this context, to know the AT release pattern from microparticles into the

Correspondence: Dr. Paz Robert, Facultad de Ciencias Químicas y Farmacéuticas, Departamento de Ciencia de los Alimentos y Tecnología Química, Universidad de Chile, Casilla 133, Santiago, Chile
E-mail: proberts@uchile.cl
Fax: 56 2 222 7900

Abbreviations: AIn, acetylated inulin; **AT,** alpha-tocopherol; **CIn,** crosslinked inulin; **DC,** degrees of cross-linking; **DP,** degree polymerization; **DS,** substitution degree; **EP,** encapsulation percentage; **FT-IR,** fourier transform infrared spectroscopy; **NIn,** native inulin; **$POCl_3$,** phosphoryl chloride

food (focus of this study) is essential, because define the applicability of microparticles. Some studies of AT release from microparticles on gastro-intestinal models have been reported [6, 8, 10, 11], but there are not AT release profile studies in foods or hydrophilic models, only one has been reported in decane [5].

Encapsulation of AT has been reported by: desolvation using gliadin [5]; ionic gelation using sodium alginate [6], β-lactoglobulin and hen egg white protein [8], β-lactoglobulin gels [10] and pectin [11]; freeze drying using maltodextrin and gelatin [7] and two studies have been reported by spray drying using pea protein, carboxymethylcellulose and their mixtures with maltodextrin [3] and native and modified soy protein isolate [12]. Spray drying is the most common method of encapsulation because of its short drying time and relatively low cost and is typically used for the preparation of dry, stable food additives, and flavors [13]. However, it is considered to be an immobilization technology rather than a true encapsulation technology, because some active compounds may be exposed superficially on the microparticle [9].

Few biopolymers are available as encapsulating agent for spray drying microencapsulation [14]. The growing interest in the inulin is due to its properties: non-toxic, biocompatible, water soluble, biodegradable, and cheap polymer [15] and it has been used mainly as a prebiotic in functional foods [16]. Inulin is a polydisperse polysaccharide consisting mainly, if not exclusively, of β-(2 → 1) fructosyl fructose units, and slightly branched fructan. The most important sources are *Cichoriumintybus* (chicory), *Dahlia pinuata Cav*. (dahlia), and *Helianthus tuberosus* (Jerusalem artichoke) which have degree polymerization (DP) of 10–14, 20, and 6, respectively [17, 18]. However, this biopolymer can be chemically modified to change its physical and chemical properties [18]. One of these modifications is the esterification of the inulin by the reaction with acetic anhydride where the hydroxyl groups of the fructose units have been esterified to acetyl groups [19–21]. Another modification is the cross-linking with bi- or polyfunctional reagents, such as phosphoryl chloride ($POCl_3$) or epichlorihydrin [18]. In this study we propose the use of native, acetylated (two substitution degrees), and cross-linked [two cross-linking degrees (CDs)] inulin as encapsulating agents of AT. There are not previous works on cross-linking of inulin and its use as encapsulating agent.

The aim of this research was to assess the effect of acetylation and cross-linking of inulin on the encapsulation percentage (EP) of these agents with AT and to evaluate the release behavior of AT from microparticles in water.

2 Materials and methods

2.1 Materials

Alpha-tocopherol 98% (AT) was obtained from Merck, Chile; sodium caseinate (SC) from Prinal and Inulin Raftilina® HP (DP>23; native inulin (NIn)) from Alfa Chile S.A.

2.2 Preparation of acetylated and cross-linked inulin

2.2.1 Acetylated inulin

Inulin acetate (AIn) was synthesized by the reaction of native inulin (10 g) with acetic anhydride (35 or 70 mL) in *N*,*N*-dimethylformamide (DMF, 100 mL) at 40°C by 24 h using sodium acetate (0.05% w/w) as catalyst, according to the method of Wu and Lee [20]. The reaction product was precipitated in an excess of cold water, recrystallized by dissolution with DMF and re-precipitation with water, and then was dried at 50°C until constant weight in an air forced oven (WTE, Germany).

2.2.2 Cross-linked inulin

Cross-linked inulin (CIn) was synthesized by reaction with $POCl_3$, according to the method described for starch by Woo and Seib [22] with some modification. Native inulin (100 g) was dispersed in water (400 mL) with constant stirring for 1 h at 25°C and then sodium sulfate (15 g) was added, followed by the addition of NaOH (1.0 M) until reached pH 11. $POCl_3$ was added drop-wise at 0.3 and 1.0% levels (based on weight inulin) maintaining the pH between 10.5 and 11.5. After 1 h, the pH was adjusted to 5.5 with HCl (1.0 M). The cross-linked inulin was precipitated with acetone, washed three times with acetone:water (60:40% v/v), and dried at 40°C by 24 h in an air forced oven (WTE, Germany).

2.3 Characterization of acetylated and cross-linked inulin

The AIn was characterized by fourier transform infrared spectroscopy (FT-IR) (Bruker, vector 22) on KBr disks and ^{1}H NMR at 400 MHz (BrukerAvance 400 Spectrometer) in deuterated dimethylsulfoxide (DMSO-d6). The quantifications of the substitution degree (DS) for inulin acetate, were determined by ^{1}H NMR spectroscopy, considering the relationship between areas of the methyl proton of the acetyl groups and those of the monomer [21].

The CIn was characterized by FT-IR on KBr disks (Bruker, vector 22), ^{31}P NMR (Bruker Avance 400 Spectrometer) in deuterated dimethylsulfoxide (DMSO-d6), and atomic emission spectroscopy (ICP-AES). The cross-linking degree was obtained considering the relationship between phosphorus moles incorporated to the polymer and the total of inulin moles [23].

2.4 Preparation of the inulin microspheres

All formulations for the native (NIn), cross-linked (CIn_1 and CIn_2), or acetylated inulin (AIn_1 and AIn_2) systems were prepared considering 100 g emulsion. NIn and CIn microspheres were obtained preparing firstly a pre-emulsion with AT (0.5 g), sodium caseinate (0.8 g) and distilled water

(20 g), which was homogenized at 20.000 rpm for 3 min with a Polytron PT 2100 (Kinematica AG, Switzerland). The encapsulating agent (5–15 g) in distilled water was heated at 55°C and then cooled until 30°C. The encapsulating solution was added on the pre-emulsion and homogenized at 20.000 rpm for 3 min. Emulsion droplet size was determined by laser light scattering in a Mastersizer X instrument (Malvern Instruments, Worcestershire, UK). In the case of AIn microparticle systems the AT (0.5 g) and encapsulating agent (5–15 g) were mixed using ethanol:water (80:20% v/v) as dissolution medium.

The resultant emulsions were fed into a B-290 mini spray dryer (Büchi, Switzerland). The spray dryer was operated at an inlet temperature ranging from 160 to 200°C for NIn and CIn systems and from 90 to 130°C for AIn systems. The air flow, rate of feeding, and atomization pressure was 600 (L/h), 2 (mL/min), and 5 bar, respectively. The powders obtained were stored to exclude light at −20°C for subsequent analysis.

2.5 Characterization of the microspheres

2.5.1 Determination of superficial and encapsulation percentage of AT

Microparticles (0.05 g) were dispersed in 2 mL of hexane (HPLC grade). These dispersions were agitated by vortexing for 1 min and then filtered (0.22 μm Millipore filter). Aliquot (200–600 μL) was placed in a 25 mLvolumetric flask and filled up with hexane and injected into the HPLC. The surface AT percentage (SP) and the AT EP were calculated according to Eqs. (1) and (2), respectively:

$$\mathrm{SP}\,(\%) = \left(\frac{\text{surface AT}}{\text{theoretical total AT}}\right) \times 100 \quad (1)$$

$$\mathrm{EP}\,(\%) = 100 - \mathrm{SP}\,(\%) \quad (2)$$

2.5.2 Chromatography procedure

The AT analysis was performed by HPLC using a Merck-Hitachi L-6200 pump (Merck, Darmstadt, Germany), injector Rheodyne 7725i, loop 20 μL and a F-1050 fluorescence detector (Merck) coupled at a computer equipped with the Clarity software. The excitation wavelength was 292 nm and the emission wavelength of 330 nm. The analytical column used was LiChrocart Superspher Si-60 (5 μm × 4 mm id × 250 mm, Merck). An isocratic mobile phase of hexane/2-propanol (99.5:0.5% v/v) was used at a flow rate of 1 mL/min [24]. AT was quantified using a calibration curve (1.05–5.25 μg/mL, $R^2 = 0.9992$).

2.5.3 Morphology microspheres

The outer structures of the microparticles obtained under optimal conditions were studied by scanning electron microscopy (SEM). The samples were coated with gold/palladium using a Varian Vacuum Evaporator PS 10E and analyzed using a LEO 1420VP (LEO Electron Microscopy, Cambridge, UK) operated at 20 kV. The scanned images were collected digitally using EDS 7424 software (Oxford Instruments, Oxford, UK).

2.6 In vitro release study

AT release profiles from AT–NIn, AT–AIn_1, AT–AIn_2, AT–CIn_1, and AT–CIn_2 microparticle systems obtained under optimal conditions were evaluated using a USP type I apparatus (Pharma Test Type PTW SIII equipment) at 25°C in 500 mL Millipore Q-Water with tween-80 (0.5% v/v) as dissolution medium. Microparticles (500 mg) in cellulose filter bags were placed into the baskets of the apparatus and rotated at 50 rpm. Aliquots of 10 mL were removed (triplicate) at specific time intervals during 9 h, and the initial volume (500 mL) was maintained by the addition of water. The release of AT was monitored by HPLC.

2.6.1 Cromatography procedure

The AT analysis was performed by HPLC using Merck-Hitachi L-6200A pump (Merck), a Waters 996 photodiode-array detector (DAD) coupled at a computer with a software Empower Pro, and a column C18 (3 μm, 4.6 mm id × 150 mm, Symmetry, Waters, Ireland). An isocratic mobile phase of methanol/acetonitrile (30:70% v/v) was used at a flow rate of 1 mL/min [25].AT detection was at 292 nm and was quantified using a calibration curve (10–100 μg/mL, $R^2 = 0.9998$).

2.7 Kinetic release analysis

The data were fitted to Higuchi kinetic models [26, 27] according to Eq. (3):

$$\frac{M_t}{M_\infty} = k \times t^{1/2} \quad (3)$$

M_t is defined as the quantity of AT released at any time t, and M_∞ is the initial AT loading of the polymer. The release rate constants (k) were obtained from the slope of a plot of M_t/M_∞ versus $(\text{time})^{1/2}$.

2.8 Statistical design

The experiments were performed with a face central composite experimental design, using spray drying as encapsulation method. Ten experiments were performed for each encapsulating agent (AT–NIn, AT–AIn_1, AT–AIn_2, AT–CIn_1, and AT–CIn_2). The AT/coating material ratios (1:10–1:30) and inlet air temperature (160–200°C for NIn and CIn and 90–130°C for AIn) were evaluated as independent variables. The AT EP was the dependent variable. The response surface

methodology was applied to optimize EP. To determine the statistical differences among AT EP, and release rate constants of the systems studied, a non-parametric tests (Kruskal–Wallis) analysis was performed. All the statistical analyses were calculated using Statgraphics Centurion XVl (StatPoint Technologies, USA, 2012).

3 Results and discussion

3.1 Characterization of acetylated and cross-linked inulin as encapsulating agents

For inulin acetates the FT-IR spectra (Fig. 1) showed that when the OH groups are substituted by acetyl groups, the OH stretch band of inulin (~3500 cm^{-1}) diminishes and the carbonyl band (C=O, ~1745 cm^{-1}) emerges. These results are similar to those reported by Wu and Lee [20] and Poulain et al. [21]. The ^{1}H NMR spectra of acetylated inulin showed the presence of a methyl singlet at $\delta = 1.93$ ppm which is absent in the native form. Depending on the amount of acetic anhydride used, two degrees of substitution (DS) were obtained for inulin acetate, 1.6 (AIn_1) and 2.1 (AIn_2). DS values were similar to those reported by Damian et al. [19] and Poulain et al. [21] with DS values of 1.8 and 1.6–2.8, respectively.

The FT-IR spectrum for cross-linked inulin (0.3 and 1% $POCl_3$; Fig. 1) showed three news signals at 620, 987, and 1200 cm^{-1} corresponding to P–C, P–O, and P=O stretching vibrations, which are absent in the native form. The phosphorus incorporation was confirmed by ^{31}P NMR spectrum for cross-linked inulin with 1% $POCl_3$, showing three signals (1.375, 0.506, and −0.635 ppm) corresponding to phosphoester vibrations ($O=P(OR)_x$). These results are similar to those reported by Yijun et al. [28] for cross-linked starch with sodium trimetaphosphate (STMP) and $POCl_3$. The phosphorus levels were determined by atomic emission spectroscopy (ICP-AES), obtaining two degrees of cross-linking (DC) of 0.052 (CIn_1) and 0.091(CIn_2). It is important to note that the Food and Drug Administration (FDA) [29] only regulates the use of $POCl_3$ for starch, with a maximum level of 0.1% (based on dry weight of starch). However, in this study were used higher levels of $POCl_3$ to obtain greater extent of changes in physicochemical properties of cross-linked inulin.

3.2 Encapsulation of alpha-tocopherol

The effect of the process and formulation variables such as inlet air temperature and AT/encapsulating agent ratio on the EP were investigated according to face central composite experimental design for each system studied.

The AT EP for AT–NIn, AT–AIn_1, AT–AIn_2, AT–CIn_1, and AT–CIn_2 ranged between 84–90%; 82–92%; 86–94%; 82–88% and 83–90%, respectively. These results show a high retention of AT with native and cross-linked inulin, which

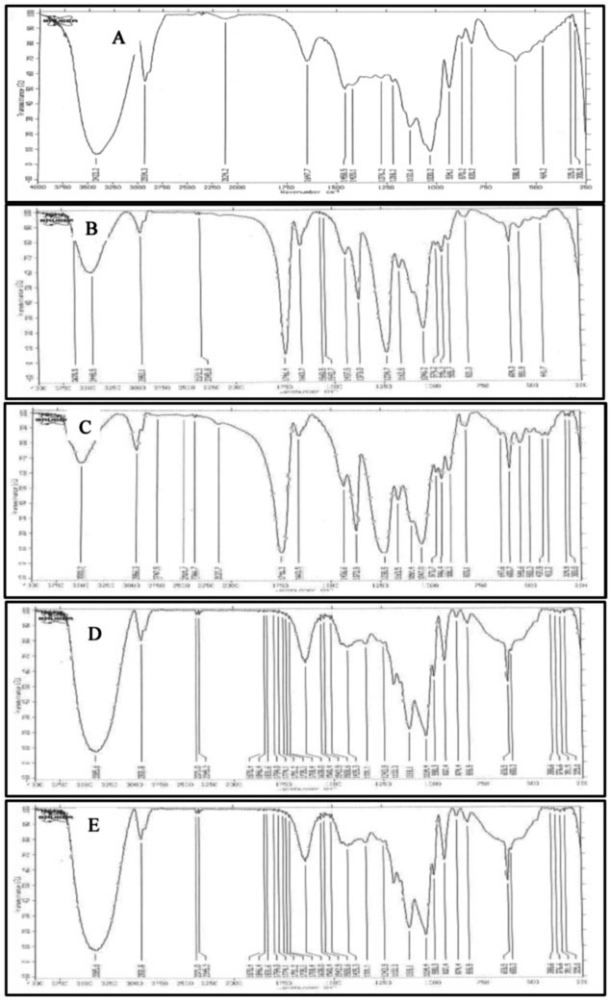

Figure 1. FT-IR spectra for AT–NIn (A), AT–AIn_1 (B), AT–AIn_2 (C), AT–CIn_1 (D), AT–CIn_2 (E).

could be attributed to the stability of feed emulsions in the spray-drying process, that play an important role on the retention of hydrophobic molecules as was reported by Pierucci et al. [3]. For achieve stable emulsions the sodium caseinate was used by its structure, a random coil with a hydrophobic head and hydrophilic tail, do it an excellent emulsifier and film former. On the other hand, the high retention in the acetylated inulin systems was attributed to the increased hydrophobicity of the polymer. The AT EP found in this research was higher than those reported with other encapsulating agents by Pierucci et al. [3] (77.8–96.7%) and Duclairoir et al. [5] (77%) using spray-drying and solvent evaporation technique, respectively. Lower encapsulation efficiency than this study was reported by Yoo et al. [6] and Somchue et al. [8] using ionic gelation.

The response surface methodology (RSM) was applied to optimize the EP of AT for each system studied, considering the linear, quadratic, and cross-product forms for independent

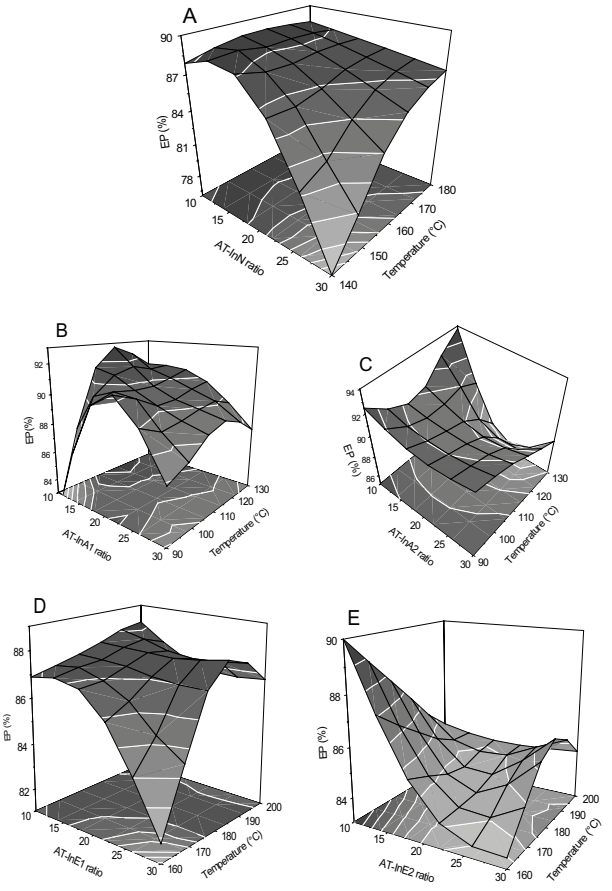

Figure 2. Graphs obtained by response surface methodology for AT–NIn (A), AT–AIn_1 (B), AT–AIn_2(C), AT–CIn_1 (D), AT–CIn_2 (E).

variables studied at $p \leq 0.05$ levels for each system. Figure 2A–E illustrates the graphs obtained with the response surface methodology for AT–NIn, AT–AIn_1, AT–AIn_2, AT–CIn_1, and AT–CIn_2 designs, respectively. The degradation of AT has been associated with oxidation and/or degradation reactions induced by heat [1], indicating the importance of inlet air temperature as a variable of the process. However, in this study a significant effect of the temperature ($p \leq 0.05$) on the AT EP was found only for linear form in AT–AIn_1 and AT–AIn_2, and for quadratic form in AT–AIn_1.

The linear and quadratic form of the AT/encapsulating agent ratio had not a significant effect ($p>0.05$) on the AT EP for the systems studied, except for AT–CIn_2, whereas the interaction between temperature and ratio was significant ($p \leq 0.05$) for AT–NIn, AT–AIn_1, and AT–CIn_2.

The optimal conditions obtained by response surface methodology, and AT encapsulating percentage for native, acetylated, and cross-linked inulin microparticles are shown in Table 1. As can be seen, different encapsulating agents have different optimum parameters in spray drying, because encapsulating agent features as solubility, viscosity among other, affects the formation rate of a crust on the particle surface [14]. The high values of AT EP (>86%) for AT–NIn, AT–CIn_1, and AT–CIn_2 systems, could be attributed to the emulsion droplet size (D 3,2) that reached values of 1.31, 1.20, and 1.65 μm, respectively, and the effect of the sodium caseinate. This results show that the emulsion properties (stability and droplet size) could be more important than the nature of encapsulating agent in encapsulation of hydrophobic molecules. In this context, has been reported that the emulsion stability is a critical step in optimizing the encapsulation efficiency [30].

In the case of AT–AIn_1 and AT–AIn_2 systems, the high values of AT EP could be attributed to hydrogen bonding between carbonyl groups (acetylated inulin) acting as material donating with hydrogen atoms of the hydroxyl groups of the tocopherol. Besides Van der Waals forces could occur too between phytyl tail and hydrophobic sites of modified inulin.

An increase in the DC and DS of cross-linked and acetylated inulin, respectively, increased significantly ($p \leq 0.05$) the AT EP in relation to NIn system. Cross-linking of inulin by reaction with $POCl_3$ generates intra- and inter-molecular bonds which form fine and dense networks structures, decreasing and preventing the AT separation during drying process, and therefore improves AT EP [14]. The incorporation of acetyl groups in the inulin, increase the hydrophobicity of the polymer promoting the interactions of hydroxyl group of AT with carbonyl group of acetylated inulin.

Figure 3A–E shows the SEM microphotograph of AT-microparticles powders obtained under optimal conditions

Table 1. Optimal conditions and encapsulation percentage in AT-microspheres with native, acetylated, and cross-linked inulin

System	AT/EA ratio	Inlet air temperature (°C)	Total theoretical AT (mg/g powder)	AT encapsulation percentage (%)
AT–NIn	1:30	200	30.9	86 ± 0.30^{a}
AT–AIn_1	1:15	126	62.8	91 ± 0.01^{b}
AT–AIn_2	1:22	90	43.6	93 ± 0.32^{c}
AT–CIn_1	1:10	180	79.6	88 ± 0.40^{b}
AT–CIn_2	1:10	160	80.6	90 ± 0.20^{c}

AIn_1, acetylated inulin (DS = 1.6); AIn_2, acetylated inulin (DS = 2.1); CIn_1, crosslinked inulin (DC = 0.052); CIn_2, crosslinked inulin (DC = 0.091); EA, encapsulating agent. Different letters show significant differences between systems ($p<0.05$).

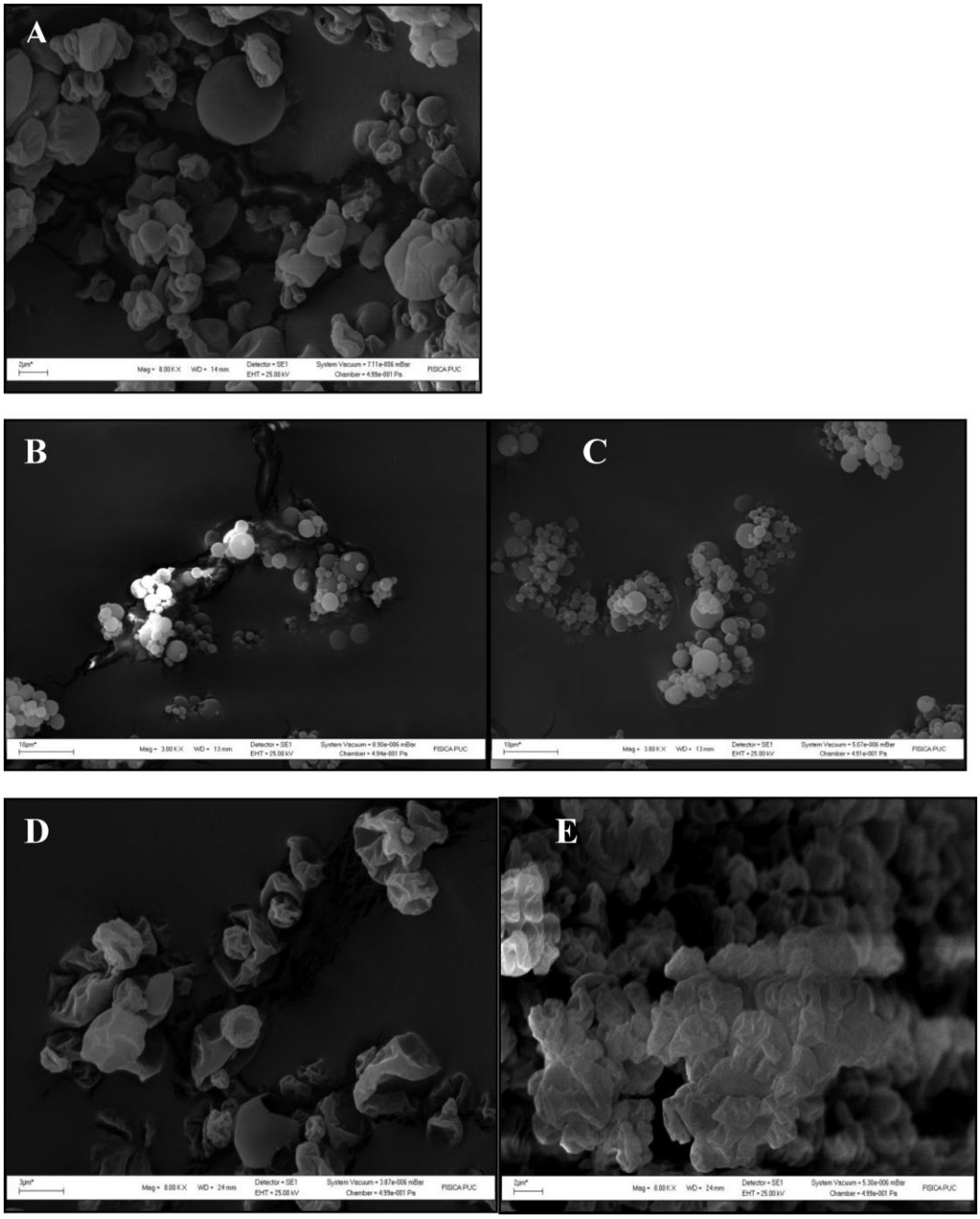

Figure 3. Scanning electron microscopic photographs for AT–NIn (A), AT–AIn$_1$ (B), AT–AIn$_2$ (C), AT–CIn$_1$ (D), AT–CIn$_2$ (E).

for all the systems studied. Microspheres of NIn (Fig. 3A) were irregular in shape, with noticeable indentation and roughness on surface of particles, which has been attributed to the shrinkage of the particles during the drying process that can occur at low or high inlet temperatures [31]. At low inlet temperatures, there is less water diffusion, and the particles have more time to shrink. At high inlet temperatures, the rapid evaporation and high pressure inside of the particles also produce shrinkage. Similar morphology was described by Ronkart et al. [32]. The AT–CIn$_1$ y AT–CIn$_2$ (Fig. 2D and E, respectively) microparticles were similar morphologically to the ones of AT–NIn, whereas the AT-acetylated inulin microspheres (Fig. 2B and C, respectively) were spherical and had homogeneous and smooth surface without indentations, showing the effect of inlet temperature and type of the solvent on the particles morphology. The tendency of

agglomeration increased with the substitution degree of the inulin.

3.3 In vitro AT release study

Figure 4A and B shows the AT release profiles from microparticles of AT-acetylated inulin (AT–AIn_1, AT–AIn_2) and AT-cross-linked inulin systems (AT–CIn_1 and AT–CIn_2) obtained under optimal conditions, using native inulin as control. The dissolution medium (water) was selected in order to simulating hydrophilic food model. Thus, 0.5% of tween-80 was added to water to improve the solubility of AT in water, as described Yoo et al. [6]. A biphasic behavior was observed in the release profile graphs (release % vs. time) for all the systems studied, in according with Poulain et al. [21] and Duclairoir et al. [5]. The first zone (0–90 min) can be attributed to the presence of uncovered AT on the surface of the microparticles (superficial AT), reaching release values $< 7\%$. A ''burst effect'' has been reported for inulin (native and acetylated) with (*E*,*E*)-bis(amidinobenzylidene)cycloheptanonein phosphate buffer (pH 7.4) [21], and wheat gliadin with AT in decane [5]. However, this effect was not observed in this study, showing that the AT diffusivity inside the matrix systems decreased due to a low solubility of AT in the dissolution medium (water + tween 80), which could be used as a method to control the release.

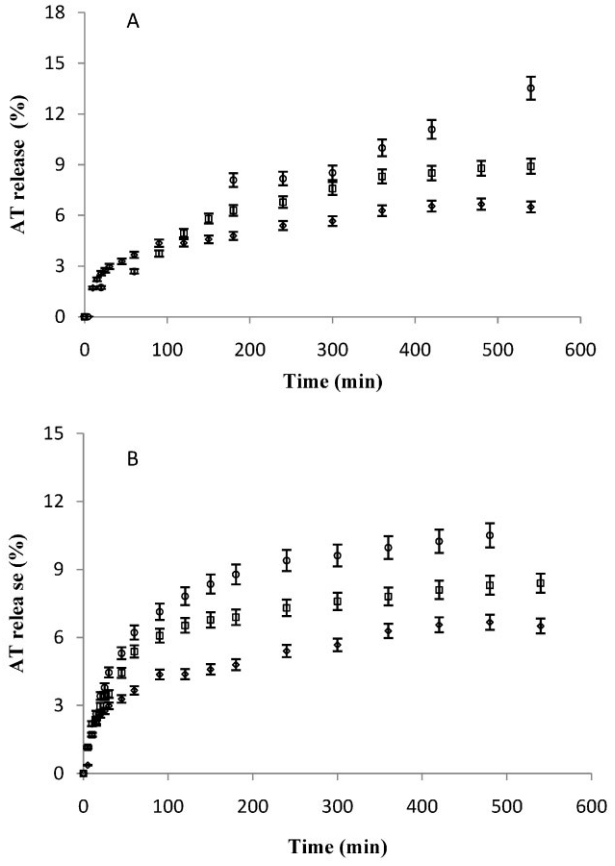

Figure 4. Release profile of alpha-tocopherol from acetylated (A) and cross-linked inulin (B) microparticles obtained under optimal conditions, in a hydrophilic model (water + tween 80) at 25°C. AT–NIn (◇), AT–AIn_1 or AT–CIn_1 (□), and AT–AIn_2 or AT–CIn_2 (○).

In the second zone, assigned to encapsulated AT release, the release was minimal, reaching values of 15% at 540 min, in agree with a very slow stage. A third phase has been reported [21] which correspond to the erosion of the inulin due to its dissolution in the medium and the total release of the encapsulated material. However, this step was not observed in this study because the release was studied for a shorter time.

According to the release profiles obtained for all the systems studied, Higuchi model was applied to explain the release mechanisms. Table 2 shows the AT release rate constants for AT with native, acetylated, and cross-linked inulin systems. The correlation coefficient showed a good fit to Higuchi model, showing that the release mechanism of AT was trough diffusional mechanism for all systems studied. AT release rate constant of AT–AIn_2 and AT–CIn_2 systems were significantly higher than those of the native inulin. This behavior could be explained because although the acetylation and cross-linking of inulin decreases the water solubility, both polymers increases their water binding capacity, facilitating the AT diffusion from microparticles to dissolution medium in comparison to non-modified inulin.

The release pattern and kinetic parameters are important for evaluating the applicability of the microparticles in foods. In cases where the release is very slow, the microparticles could be used for the formulation of functional foods. Conversely, when microencapsulated bioactive compounds have fast release kinetics, the active compound becomes exposed to the food matrix, losing its protection. According to release profiles of AT, all the AT-inulin microparticles studied could be applied to formulation of functional foods. However, it is important to note that

Table 2. AT release rate constants obtained from release curves for AT-microparticles with native, acetylated, and cross-linked inulin

System	Higuchi 10^2 k ± 10^2 SD ($min^{-0.5}$)	R^2
AT–InN	0.24 ± 0.01^{c}	0.969
AT–AIn_1	0.36 ± 0.03^{bc}	0.943
AT–AIn_2	0.56 ± 0.09^{a}	0.962
AT–CIn_1	0.33 ± 0.01^{bc}	0.900
AT–CIn_2	0.46 ± 0.01^{ab}	0.919

AIn_1, acetylated inulin (DS = 1.6); AIn_2, acetylated inulin (DS = 2.1); CIn_1, crosslinked inulin (DC = 0.052); CIn_2, cross-linked inulin (DC = 0.091); EA, encapsulating agent. Different letters show significant differences between systems ($p < 0.05$).

differences in the release pattern of AT could be observed with other dissolution medium.

4 Conclusion

Native, acetylated, and cross-linked inulin showed a high AT EP (>86%) due to AT-polymer interaction and/or emulsion properties. The release profile of AT from microparticles in a hydrophilic system (water + tween 80) showed that the all systems studied released mainly the uncovered AT, according to diffusional mechanism (Higuchi model). These results suggest that the microparticles could be applied in formulation of functional foods, preserving AT nutritional properties.

This work was part of Grant N° 1090209 from The National Fund for Scientific and Technological Development (Fondecyt, Chile).

The authors have declared no conflict of interest.

References

[1] Kamal-Eldin, A., Appelqvist, L., The chemistry and properties of tocopherols and tocotrienols. *Lipids* 1996, *31*, 671–701.

[2] Brigelius-Flohé, A., Traber, M., Vitamin E: Function and metabolism. *J. Fed. Am. Soc. Exp. Biol. (FASEB)* 1999, *13*, 1145–1155.

[3] Pierucci, A., Andrade, L., Farina, M., Pedrosa, C., Comparison of α-tocopherol microparticles produced with different wall materials: Pea protein a new interesting alternative. *J. Microencapsul.* 2007, *24*, 201–213.

[4] Talegawkar, S., Johnson, E., Carithers, T., Taylor, H. et al., Total α-tocopherol intakes are associated with serum α-tocopherol concentrations in African American adults. *J. Nutr.* 2011, *23*, 2297–2303.

[5] Duclairoir, C., Orecchiomi, A. M., Depraetere, P., Nakache, E., α-Tocopherol encapsulation and in vitro release from wheat gliadin nanoparticles. *J. Microencapsul.* 2002, *19*, 53–60.

[6] Yoo, S. H., Song, Y. B., Chang, P. S., Lee, H. G., Microencapsulation of alpha-tocopherol using sodium alginate and its controlled release properties. *Int. J. Biol. Macromol.* 2006, *38*, 25–30.

[7] Farias, M., Moura, M., Andrade, L., Rocha, M. H., Encapsulation of the alpha-tocopherol in a glassy food model matrix. *Mater. Res.* 2007, *10*, 57–62.

[8] Somchue, W., Sermsri, W., Shiowatana, J., Siripinyanond, A., Encapsulation of α-tocopherol in protein-based delivery particles. *Food Res. Int.* 2009, *42*, 909–914.

[9] De Vos, P., Faas, M., Spasojevic, M., Sikkema, J., Encapsulation for preservation of functionality and targeted delivery of bioactive food components. *Int. Dairy J.* 2010, *20*, 292–302.

[10] Liang, L., Leung, V., Remondetto, G., Subirade, M., In vitro release of α-tocopherol from emulsion-loaded β-lactoglobulins gel. *Int. Dairy J.* 2010, *20*, 176–181.

[11] Song, Y., Lee, J., Gyu, H., α-Tocopherol-loaded Ca-pectinate microcapsules: Optimization, in vitro release and bioavailability. *Colloids Surf. B: Biointerfaces* 2009, *73*, 394–398.

[12] Nesterenko, A., Alric, I., Silvestre, F., Durrieu, V., Influence of soy protein's structural modification on their microencapsulation properties: α-Tocopherol microparticle preparation. *Food Res. Int.* 2012, *48*, 387–396.

[13] Desai, K. G., Park, H. J., Recent developments in microencapsulation of food ingredients. *Dry. Technol.* 2005, *23*, 1361–1394.

[14] Gharsallaoui, A., Roudaut, G., Chambin, O., Voilley, A., Saurel, R., Applications of spray-drying in microencapsulation of food ingredients: An overview. *Food Res. Int.* 2007, *40*, 1107–1121.

[15] Tripodo, G., Pitarresi, G., Palumbo, F. S., Craparo, E. F., Giammona, G., UV-photocrosslinking of inulin derivatives to produce hydrogels for drug delivery application. *Macromol. Biosci.* 2005, *5*, 1074–1084.

[16] Kun-Nan, Ch., Ming-Ju, Ch., Je-Ruei, L., Chin-Wen, L., Hsin-Yi, Ch., Optimization of incorporated prebiotics as coating materials for probiotic microencapsulation. *J. Food Sci.* 2005, *70*, 260–266.

[17] Rusu, G., Bandur, G., Manoviciu, I., Rusnac, L., Plesu, N., Solubility and viscosity studies on inulin modified with methacyloyl and palmitoyl chlorides. *Chem. Bull. "Politehnica" Univ. (Timişoara)* 2006, *51*, 83–86.

[18] Stevens, C., Meriggi, A., Booten, K., Chemical modification of inulin, a valuable renewable resource and its industrial applications. *Biomacromolecules* 2001, *2*, 1–15.

[19] Damian, F., Van Den Mooter, G., Samyn, C., Kinget, R., In vitro biodegradation study of acetyl and methyl inulins by *Bifidobacteria* and inulinase. *Eur. J. Pharm. Biopharm.* 1999, *47*, 275–282.

[20] Wu, X. Y., Lee, P. I., Preparation and characterization of inulin ester microspheres as drug carriers. *J. Appl. Polym. Sci.* 2000, *77*, 833–840.

[21] Poulain, N., Dez, I., Perrio, C., Lasne, M.-C. et al., Microspheres based on inulin for the controlled release of serine protease inhibitors: Preparation, characterization and in vitro release. *J. Control. Release* 2003, *92*, 27–38.

[22] Woo, K. S., Seib, P. A., Cross-linked resistant starch: Preparation and properties. *Cereal Chem.* 2002, *79*, 819–825.

[23] Van Hung, P., Morita, N., Effects of granule sizes on physicochemical properties of cross-linked and acetylated wheat starches. *Starch* 2005, *57*, 413–420.

[24] AOCS, in: *Official Methods of Recommended Practices of the American Oil Chemists' Society*, 4th Edn., AOCS Press, Champaign 1993, Method Ce8-89.

[25] Sánchez-Machado, D. I., López-Hernandez, J., Paseiro-Losada, P., High perfomance liquid chromatographic determination of α-tocopherol in microalgae. *J. Chromatogr.* 2002, *976*, 277–284.

[26] Higuchi, T., Mechanism of sustained-action medication. Theoretical analysis of rate of release of solid drugs dispersed in solid matrices. *J. Pharm. Sci.* 1963, *52*, 1145–1149.

[27] Pothakamury, U. R., Barbosa-Cánovas, G. V., Fundamental aspect of controlled release in foods. *Trends Food Sci. Technol.* 1995, *6*, 397–406.

[28] Yijun, S., Prakash, O., Seib, P., Characterization of phosphorylated cross-linked resistant starch by ^{31}P nuclear

magnetic resonance (^{31}P-NMR) spectroscopy. *Carbohydr. Polym.* 2007, *67*, 201–212.

[29] Food and Drug Administration, 21 Code of Federal Regulations 172.892. 1995.

[30] Jafari, S., He, Y., Bhandari, B., Effectiviness of encapsulating biopolymers to produce sub-micron emulsions by high energy emulsification techniques. *Food Res. Int.* 2007, *40*, 862–873.

[31] Alamilla-Beltrán, L., Chanona-Pérez, J. J., Jimenez-Aparicio, A. R., Gutierrez-López, G. F., Description of morphological changes of particles along spray drying. *J. Food Eng.* 2005, *67*, 179–184.

[32] Ronkart, S., Deroanne, C., Paquot, M., Fougnies, C. et al., Characterization of the physical state of spray-dried inulin. *Food Biophys.* 2007, *2*, 83–92.

